Hydrological Sciences Journal
Publication details, including instructions for authors and subscription information:
http://www.tandfonline.com/loi/thsj20

Analysis of hydrological seasonality across northern catchments using monthly precipitation-runoff polygon metrics

Genevieve Ali[a], Doerthe Tetzlaff[b], Laura Kruitbos[c], Chris Soulsby[b], Sean Carey[d], Jeff McDonnell[be], Jim Buttle[f], Hjalmar Laudon[g], Jan Seibert[h], Kevin McGuire[i] & Jamie Shanley[j]

[a] Department of Geological Sciences, University of Manitoba, Manitoba, Canada
[b] Northern Rivers Institute, School of Geosciences, University of Aberdeen, Scotland, UK
[c] School of Biological Sciences, University of Aberdeen, Scotland, UK
[d] School of Geography and Earth Sciences, McMaster University, Ontario, Canada
[e] Global Institute for Water Security, University of Saskatchewan, Saskatchewan, Canada
[f] Department of Geography, Trent University, Ontario, Canada
[g] Department of Forest Ecology and Management, SLU, Umeå, Sweden
[h] Department of Geography, University of Zurich - Irchel, Zurich, Switzerland
[i] Virginia Water Resources Research Center, Virginia Tech, Blacksburg, VA, USA
[j] US Geological Survey, Montpelier, VT, USA

Accepted author version posted online: 05 Jul 2013.Published online: 25 Nov 2013.

http://dx.doi.org/10.1080/02626667.2013.822639

Analysis of hydrological seasonality across northern catchments using monthly precipitation–runoff polygon metrics

Genevieve Ali[1], Doerthe Tetzlaff[2], Laura Kruitbos[3], Chris Soulsby[2], Sean Carey[4], Jeff McDonnell[2,5], Jim Buttle[6], Hjalmar Laudon[7], Jan Seibert[8], Kevin McGuire[9] and Jamie Shanley[10]

[1]*Department of Geological Sciences, University of Manitoba, Manitoba, Canada*
Genevieve.Ali@umanitoba.ca

[2]*Northern Rivers Institute, School of Geosciences, University of Aberdeen, Scotland, UK*

[3]*School of Biological Sciences, University of Aberdeen, Scotland, UK*

[4]*School of Geography and Earth Sciences, McMaster University, Ontario, Canada*

[5]*Global Institute for Water Security, University of Saskatchewan, Saskatchewan, Canada*

[6]*Department of Geography, Trent University, Ontario, Canada*

[7]*Department of Forest Ecology and Management, SLU, Umeå, Sweden*

[8]*Department of Geography, University of Zurich – Irchel, Zurich, Switzerland*

[9]*Virginia Water Resources Research Center, Virginia Tech, Blacksburg, VA, USA*

[10]*US Geological Survey, Montpelier, VT, USA*

Received 26 September 2012; accepted 2 June 2013; open for discussion until 1 July 2014

Editor Z.W. Kundzewicz; **Associate editor** K. Heal

Citation Ali, G., Tetzlaff, D., Kruitbos, L., Soulsby, C., Carey, S., McDonnell, J., Buttle, J., Laudon, H., Seibert, J., McGuire, K., and Shanley, J., 2013. Analysis of hydrological seasonality across northern catchments using monthly precipitation–runoff polygon metrics. *Hydrological Sciences Journal*, 59 (1), 1–17.

Abstract Seasonality is an important hydrological signature for catchment comparison. Here, the relevance of monthly precipitation–runoff polygons (defined as scatter points of 12 monthly average precipitation–runoff value pairs connected in the chronological monthly sequence) for characterizing seasonality patterns was investigated to describe the hydrological behaviour of 10 catchments spanning a climatic gradient across the northern temperate region. Specifically, the research objectives were to: (a) discuss the extent to which monthly precipitation–runoff polygons can be used to infer active hydrological processes in contrasting catchments; (b) test the ability of quantitative metrics describing the shape, orientation and surface area of monthly precipitation–runoff polygons to discriminate between different seasonality patterns; and (c) examine the value of precipitation–runoff polygons as a basis for catchment grouping and comparison. This study showed that some polygon metrics were as effective as monthly average runoff coefficients for illustrating differences between the 10 catchments. The use of precipitation–runoff polygons was especially helpful to look at the dynamics prevailing in specific months and better assess the coupling between precipitation and runoff and their relative degree of seasonality. This polygon methodology, linked with a range of quantitative metrics, could therefore provide a new simple tool for understanding and comparing seasonality among catchments.

Key words precipitation–runoff dynamics; monthly time scale; polygons; seasonality; North-Watch project Canada; catchment inter-comparison

Analyse de la saisonnalité hydrologique sur des bassins versants septentrionaux à l'aide de métriques de polygones précipitation–débit mensuels

Résumé La saisonnalité est une signature hydrologique importante pour la comparaison de bassins. Ici, nous avons étudié la pertinence de polygones précipitation-débit mensuels (définis dans le plan à partir des points représentatifs de 12 paires de valeurs précipitation-débit moyen mensuel reliés par des segments de droite selon l'ordre chronologique des mois), à caractériser la saisonnalité du comportement hydrologique de 10 bassins versants couvrant un gradient climatique à travers les régions tempérées du Canada septentrional. Plus précisément, les objectifs de la recherche étaient: (a) d'examiner dans quelle mesure les polygones précipitation-débit mensuels pouvaient être utilisés pour inférer les processus hydrologiques actifs dans des bassins versants contrastés, (b) de tester la capacité de métriques décrivant la forme, l'orientation et la surface des polygones précipitation-débit mensuels à discriminer différents modes de saisonnalité, et (c) d'apprécier la valeur des polygones précipitation-débit comme base d'un regroupement et d'une comparaison des bassins. Cette étude a montré que certaines métriques des polygones étaient aussi efficaces que les coefficients d'écoulement mensuel moyens pour caractériser les différences entre les 10 bassins versants. L'utilisation des polygones précipitation-débit a été particulièrement utile pour examiner les dynamiques prévalant certains mois et pour mieux évaluer le couplage entre les précipitations et l'écoulement et leur degré relatif de la saisonnalité. Cette méthodologie des polygones, en lien avec une série de mesures quantitatives, pourrait donc fournir un nouvel outil simple pour comprendre et comparer la saisonnalité entre bassins.

Mots clefs dynamique précipitation-débit; pas de temps mensuel; polygones; saisonnalité; projet North-Watch; Canada; comparaison de bassins

1 INTRODUCTION

Catchments around the world are characterized by varying degrees of seasonality when it comes to the timing, volume, intensity, frequency and duration of precipitation and runoff (Xiong *et al.* 2006, Carey *et al.* 2010, Tetzlaff *et al.* 2010, La Torre Torres *et al.* 2011). Here, seasonality is defined as the presence of regular and predictable oscillations in a given time series which recur every calendar year. Given that climate variability influences both storm characteristics (e.g. Vidon *et al.* 2009) and soil moisture (e.g. Western *et al.* 2002, Wilson *et al.* 2004), patterns of seasonality provide an important control on time-variable processes of runoff generation and climate change impact. This applies especially in mountain or high-latitude areas (Parajka *et al.* 2009), where the elevation of the zero-degree isotherm plays a critical role in determining the phase of precipitation as well as snow storage (Carey *et al*. 2010). Seasonality is also considered to be an important hydrological signature for catchment classification or regionalization studies, as it can help identify regions with similar hydrological response (Castellarin *et al.* 2001, Woods 2003, Laaha and Blöschl 2006, Parajka *et al.* 2009, Jothityangkoon and Sivapalan 2009). Thus, many recent hydrological studies (e.g. Laaha and Blöschl 2006, Carey *et al*. 2010, Bartolini *et al.* 2011) have focused on quantifying seasonality in both precipitation and runoff, not only for process understanding but also for catchment comparison purposes.

Many different methodologies have been tested to quantify the degree of seasonality in a catchment, from purely statistical indices to indices derived from geometrical approaches. The Pardé coefficient, seasonality histograms and the seasonality ratio have been some of the most effective statistical approaches. The Pardé coefficient (Pardé 1947) describes the seasonality of mean monthly precipitation and runoff, and ranges from 1 to 12, where a value of 1 represents a uniformly distributed variable throughout the year, whereas a value of 12 means that all precipitation or runoff occurs within a single month. Laaha and Blöschl (2006) used seasonality histograms to quantify the monthly distribution of low flows (i.e. Q_{95} flow quantile), especially their multi-modality and asymmetry. Both the Pardé coefficient and seasonality histograms are useful proxies for catchment runoff regime, as they rely on the sequence of monthly values (Bartolini *et al*. 2011). The seasonality ratio has been used to quantify the ratio of summer and winter low flows, as they reflect different underlying hydrological processes driving the transformation of precipitation into runoff at different times of the year (Laaha and Blöschl 2006). Carey *et al.* (2010) also derived a range of normalized fluxes and standard flow metrics, such as the coefficient of variation of monthly precipitation, to quantify the degree of seasonality present in 10 experimental catchments to formalize inter-comparison. The most commonly used geometrical approach to quantify seasonality is the Burn index (Burn 1997), which defines the mean date and variability of occurrence of extreme events. As such, it is useful for examining the seasonality of the maximum annual runoff or the annual maximum daily precipitation. Laaha and Blöschl (2006) used a cyclic seasonality index, which is similar to the Burn index, except that it describes the average timing of low flows over a year.

Here, the focus is on another geometrical approach, namely, precipitation–runoff polygons, which can assist in seasonality analysis and bear one significant advantage over the approaches previously outlined. While most of the statistical or geometrical indices of seasonality deal with precipitation and runoff in isolation, the methodology of Kadioglu and Sen (2001) plots monthly average precipitation values (on the *y*-axis) and associated monthly average runoff values (on the *x*-axis) on the same diagram with a rectangular coordinate system. Note that the graphic representation in Fig. 1(a) plots monthly average precipitation values on the *x*-axis and associated monthly average runoff values

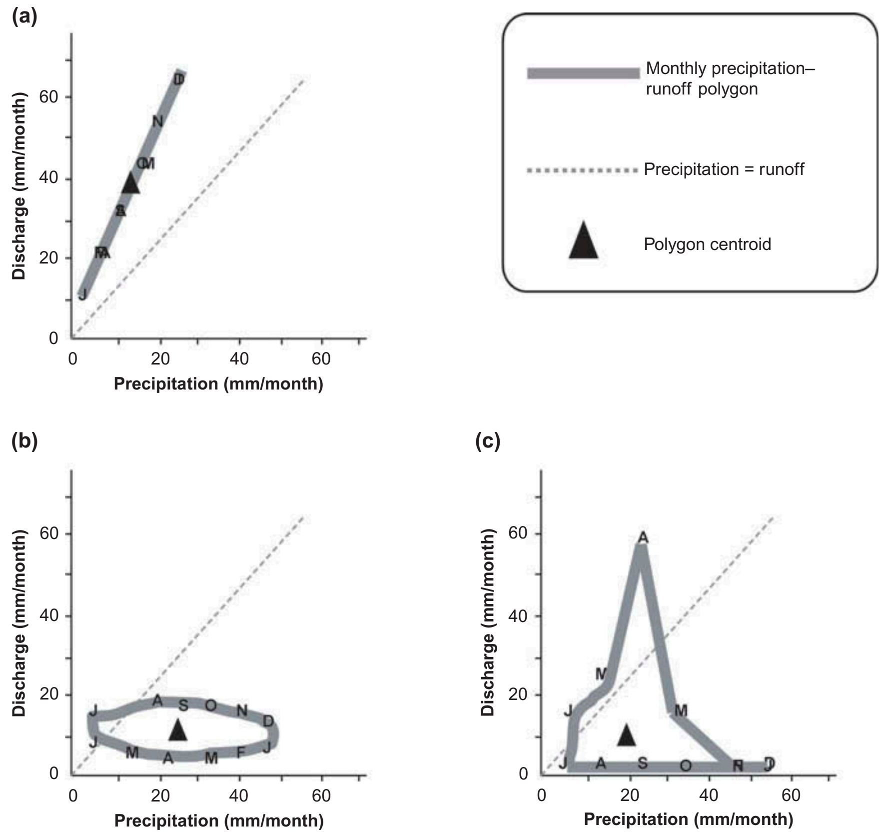

Fig. 1 Examples of monthly precipitation–runoff polygons associated with idealized runoff regimes: (a) direct runoff; (b) baseflow-dominated and (c) snowmelt-dominated behaviours. The letters J to D on each polygon vertex represent the 12 months of the year. Here, a "direct runoff" behaviour is a linear one with a constant precipitation to runoff transformation factor.

on the *y*-axis; this is contrary to Kadioglu and Sen (2001), but more intuitive. Once a scatter plot is obtained with 12 points representing monthly average precipitation–runoff value pairs, an irregular polygon is obtained by connecting the points in the chronological monthly sequence (Kadioglu and Sen 2001, Sen and Altunkaynak 2006). This polygon representation is more informative than the typical sub-monthly precipitation–runoff scatter diagram, as the latter does not inform about seasonal variability and is often associated with a linear regression line between the two variables (e.g. Hoyt 1936), thus implying that the conversion of precipitation into runoff occurs according to a constant transformation factor at all time scales (Kadioglu and Sen 2001). Alternatively, the polygon methodology only assumes a constant transformation factor between precipitation and runoff for individual months, but not at the annual scale; the variability in precipitation–runoff processes at the annual scale is indeed reflected in the fact that all polygon sides do not have the same orientation (Kadioglu and Sen 2001, Fig. 1).

Both Kadioglu and Sen (2001) and Sen and Altunkaynak (2006) suggested the use of monthly precipitation–runoff polygons for understanding catchment hydrological response using a series of process interpretations (see Table 2 and the associated discussion below). However, to date, no body of work has discussed the usefulness of these process interpretations for seasonality analysis, nor their generalization for an array of catchments wider than the one used by Kadioglu and Sen (2001) and Sen and Altunkaynak (2006). The qualitative aspect of the process interpretations used by Kadioglu and Sen (2001) and Sen and Altunkaynak (2006) also hinders their potential for comparing inter-catchment differences; no quantitative metrics or indices have been developed in association with these process interpretations to standardize the use of precipitation–runoff polygons. Hence, it is suggested to reinforce the qualitative analytical framework of the polygon approach by discussing the conclusions which can indeed be drawn from this geometrical approach and by matching each process interpretation with a set of metrics describing the shape of the geometric forms.

Here, we investigate the usefulness and relevance of monthly precipitation–runoff polygons for seasonality analysis for comparison of experimental sites. We take advantage of the 10 North-Watch (Northern Watershed Ecosystem Response to Climate Change, http://www.abdn.ac.uk/northwatch) catchments for this analysis—among the most intensively studied long-term research catchments across the circumboreal region. North-Watch is an international inter-comparison project which seeks to study the comparative hydrology of experimental sites in the northern-temperate, boreal, subarctic region that are experiencing or are sensitive to climate change, using a space-for-time substitution. The network comprises 10 experimental catchments across different hydro-climatic zones within Scotland, Sweden, Canada and the United States, and spans a climatic gradient across the northern temperate region (mean annual temperatures range from –2.1°C to 9.2°C, and mean annual precipitation ranges from 478 to 2632 mm, Table 1). A previous study done in the North-Watch catchments (Carey *et al*. 2010) established important differences among the sites in relation to seasonality. Two statistical measures or “seasonality metrics” were used, namely, the coefficient of variation of all monthly precipitation values, and the coefficient of variation of all monthly discharge. The former provided information on the magnitude of difference between wet and dry seasons, while the latter indicated the magnitude of seasonal flow variability. Among the North-Watch catchments, four were shown not to exhibit distinct wet and dry seasons, three were shown to have distinct wet and dry seasons and one had a year-long wet season. High seasonality in monthly discharge was also found for catchments with a hydrological regime dominated by a large spring snowmelt; however, the seasonality metrics chosen for that analysis had a limited potential to illustrate high flow seasonality (i.e. high standard deviation of flow) when the magnitude of the flows was also high (i.e. high average of flow). The Carey *et al.* (2010) paper not only called for further work on seasonality metrics, but also established that seasonality does exist across the North-Watch network, thus making it appropriate for this study which aims to determine whether monthly precipitation–runoff polygons can be used for seasonality analysis. Specifically, the objectives of this paper are to: (a) discuss the extent to which monthly precipitation–runoff polygons can be used to infer active hydrological processes in contrasting catchments, (b) test the ability of quantitative metrics describing the shape, orientation and surface area of monthly precipitation–runoff polygons to discriminate between different seasonality patterns; and (c) examine the value of precipitation–runoff polygons as a basis for catchment comparison. Polygon metrics are notably compared with other more conventional hydrological metrics, such as the runoff coefficient, with regard to their power to discriminate between different seasonality patterns among the study sites. The 10 North-Watch sites provide a meaningful set of catchments to test the polygon methodology and examine whether it can help us to understand their similarities and differences in seasonal behaviour. In contrast to other site-comparisons without prior detailed process understanding, empirical knowledge of the hydrological and biogeochemical behaviour of the North-Watch catchments is therefore compared with the results of the simple polygon methodology to assess whether the latter methodology is informative and reliable when it comes to characterizing catchment hydrological response at the seasonal time scale.

2 NORTH-WATCH STUDY CATCHMENTS

The characteristics of the 10 North-Watch sites have been discussed in detail by Carey *et al.* (2010) and Kruitbos *et al.* (2012) and are summarized in Table 1. Briefly, the catchments span different hydroclimatic zones, including northern temperate, subarctic and boreal environments, providing an inter-comparison framework across the circumboreal region (Fig. 2). The three Scottish catchments, of 8–30 km^2 in area are: Strontian situated in the maritime northwest, the Allt a’Mharcaidh in the western subarctic Cairngorms and the Girnock in the northeast. Mean annual temperature for the Scottish catchments ranges from 5.7°C to 9.1°C, and the geology consists largely of igneous and metamorphic rocks (Robins 1990). Vegetation cover at these Scottish sites is predominantly *Pinus sylvestris* on lower slopes, especially at Strontian, while heather (*Calluna* spp.) is present on steeper slopes at higher altitudes, and blanket bog (*Sphagnum* spp.) in poorly drained areas (Bayfield and Nolan 1998).

The Swedish site, the Krycklan catchment (Site 7, 0.50 km^2), is located on the Fennoscandian shield. It has a mean annual temperature of 2.4°C and is the second driest of all North-Watch catchments with

Table 1 Selected hydroclimatic and terrain characteristics of the 10 North-Watch study catchments.

Country	Catchment	Site	Coded name	Area (km^2)	Mean altitude (m)	Relief (m)	Precipitation (mm $year^{-1}$)	Runoff (mm $year^{-1}$)	Annual runoff ratio (–)	Baseflow index (–)
Scotland	Allt a'Mharcaidh	Site 1	MHA	10	704	779	1222	873	0.72	0.54
	Girnock	Littlemill	GIR	30	405	620	1059	603	0.57	0.38
	Strontian	Polloch	STR	8	340	740	2632	2213	0.84	0.21
Canada	Catamaran Brook	Middle Reach	CAT	28.7	210	260	990	534	0.54	0.58
	Dorset	Harp 5	DOR	1.9	373	93	980	577	0.55	0.37
	Wolf Creek	Granger Basin	WOL	7.6	1700	750	478	352	0.74	0.67
Sweden	Krycklan	Svartberget	KRY	0.5	280	72	651	327	0.49	0.47
USA	HJ Andrews	Mack Creek	HJA	5.81	1200	860	2158	1744	0.80	0.51
	Hubbard Brook	W3	HUB	0.41	642	210	1381	882	0.63	0.33
	Sleepers River	W9	SLE	0.41	604	167	1256	743	0.59	0.54

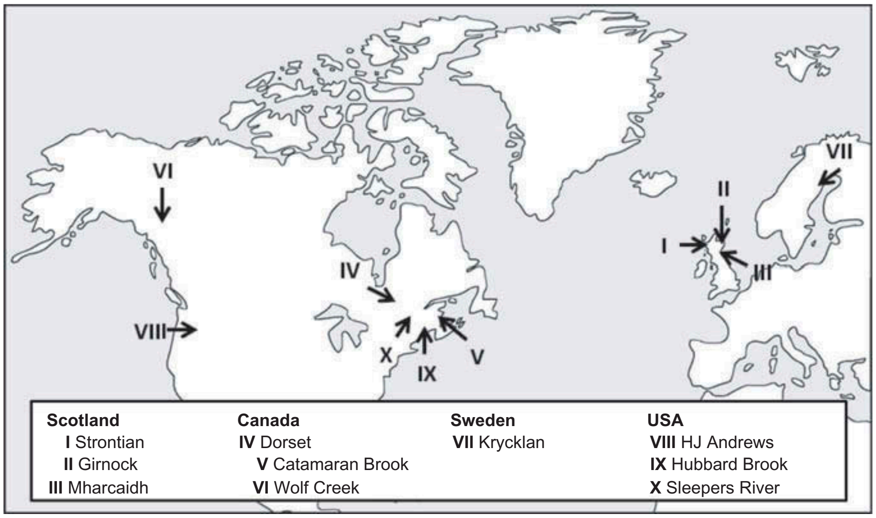

Fig. 2 Location of the 10 North-Watch study catchments.

annual precipitation of 651 mm, of which 40% falls as snow. The catchment is primarily forested with mature Scots Pine (*Pinus sylvestris*) in dry upslope areas and Norway Spruce (*Picea abies*) in wetter, low-lying areas (Laudon *et al.* 2011). *Sphagnum*-rich wetlands also dominate flatter portions in the landscape, which experience substantial soil frost during winters.

The Canadian study sites are Dorset (Harp 5, 1.19 km^2, Ontario), Wolf Creek (Granger basin, 7.6 km^2, Yukon Territory) and Catamaran Brook (Middle Reach, 28.7 km^2, New Brunswick). Dorset is at the transition to the southern boreal ecozone (Eimers *et al.* 2008). It has a humid continental climate with a mean annual temperature of 4.9°C and 980 mm of precipitation. Soil frost is rare, occurring primarily in wetlands during most winters. Vegetation is deciduous or mixed forest on well-drained soils, whilst poorly drained soils have mixed or coniferous forest. The Wolf Creek site, located on the fringe of the Coast Mountains of Yukon, is the coldest and driest of the 10 North-Watch catchments, with a mean annual air temperature of –2.12°C. It has a characteristic subarctic continental climate, where permafrost underlies 70% of the catchment and annual precipitation is low (478 mm). The geology is primarily sedimentary, comprised of limestone, sandstone, siltstone and conglomerate, overlain by a mantle of glacial till of 1–4 m thickness (Carey and Quinton 2005). Vegetation consists of shrubs (*Salix*) and alpine tundra at higher elevations (McCartney *et al.* 2006). Catamaran Brook catchment (28.7 km^2) is a third-order tributary stream of the Miramichi River in central New Brunswick and it is geologically characterized as Palaeozoic volcanic and sedimentary basement overlain by glaciofluvial deposits of loamy to sandy loam texture (Bouchard and Jolicoeur 2000). Forest cover is predominantly second-growth, southern boreal species such as white spruce (*Picea glauca)*, balsam fir (*Abies balsamea)*, birch (*Betula papyrifera*) and maple (*Acer rubrum*). Mean annual precipitation is 990 mm, with a mean annual air temperature of 5°C.

Lastly, the three catchments in the USA are Hubbard Brook in the White Mountains of New Hampshire, Sleepers River in northeastern Vermont and HJ Andrews in Oregon in the Pacific Northwest. Hubbard Brook Experimental Forest (WS3, 0.41 km^2) is covered by second-growth northern hardwood species. It has a humid continental climate with short, cool summers and long, cold winters (Likens and Bormann 1995, Bailey *et al.* 2003). Mean annual air temperature is 6.4°C, and precipitation is 1381 mm. The geology of the catchment is mainly composed of pelitic schist overlain by basal and ablation tills of varying thickness. Sleepers River (W9, 0.41 km^2) has a mean annual air temperature of 4.7°C and receives about 1256 mm of precipitation annually, of which ~25% falls as snow. The catchment is primarily forested with northern hardwoods of sugar maple, ash, beech and yellow birch (Shanley and Chalmers 1999). Agricultural land and softwoods of red spruce, balsam fir, tamarack, hemlock and white cedar also dominate. Bedrock mostly consists of quartz-mica phyllite with calcareous granulite overlain by dense silty till. The 5.8-km^2 Mack Creek catchment, located in the HJ Andrews experimental forest, is the steepest catchment with the highest relief (860 m). The geology is composed of andesitic and basaltic lava flows, and the catchment is mostly covered by old growth Douglas fir (*Pseudotsuga menziesii*) forest. Climate is characterized by wet mild winters and warm dry summers (Anderson 1992) and it is the warmest and wettest of the 10 study catchments, with a mean annual air temperature of 9.2°C and mean annual precipitation of 2158 mm.

3 POLYGON METHODOLOGY

3.1 North-Watch catchment data

Long-term hydroclimatic data for each of the study catchments were collected and compiled by the North-Watch network. The database includes daily time series of various lengths of multiple variables, such as air temperature, precipitation and discharge. To facilitate inter-site comparison, a common 10-year study period (1998–2008) was chosen for all sites except for the Allt a'Mharcaidh (4 years) and Catamaran Brook (6 years). For the purpose of comparing seasonality among the sites, monthly precipitation–runoff polygons were defined. For this, monthly averages of precipitation and runoff were calculated and standardized on a 0–1 scale by dividing the average value for each month by the yearly average maximum monthly value for each catchment. These values (precipitation *vs* runoff) were then plotted as 12 points that were connected in the chronological monthly sequence to obtain a polygon for each catchment.

3.2 Polygon-related process interpretations

The goal of this study was to assess the potential of monthly precipitation–runoff polygons to serve as effective tools for catchment seasonality analysis and to inform on active precipitation–runoff transformation processes. Both Kadioglu and Sen (2001) and Sen and Altunkaynak (2006) have suggested a series of process interpretations, as reported in Table 2, although their formulation has never been challenged outside of the context in which they were developed. Here, we discuss those interpretations and evaluate the adequate polygon metrics that should be defined in association with those interpretations.

Several process interpretation rules focus on precipitation–runoff behaviour from month to month, such as the one concerning the change in average values of precipitation and runoff (Rule (a) in Table 2) for consecutive months. Kadioglu and Sen (2001) and Sen and Altunkaynak (2006) argued that this average change was illustrated in the length of the polygon sides; however, we find this statement to be incomplete, as it does not account for cases where we could have two sides of the same length, one vertical and one horizontal, which refer to very different precipitation and runoff dynamics. We therefore rephrased this rule to underline the importance of both the length and the slope of the polygon sides to quantify the average changes. The slopes of the polygon sides are also found to be informative on the difference in runoff between months relative to the difference in precipitation between months (Rule (b) in Table 2). Both Kadioglu and Sen (2001) and Sen and Altunkaynak (2006) used their polygons to draw inferences about the linearity of the relationship between precipitation and runoff (Rule (d) in Table 2); however, we find that such an assumption of critical, complex behaviour is difficult to conceptualize at the monthly time scale. Here, we rather consider a revised process interpretation driven by the width of the polygons: a narrow one indicates a more consistent monthly runoff–precipitation relationship between months, while a wide one indicates substantial between-month differences in the runoff–precipitation relationship that may reflect variability in factors such as evapotranspiration, and retention and release of precipitation. With regard to the characterization of seasonality, one of the most interesting process interpretations put forward by Kadioglu and Sen (2001) and Sen and Altunkaynak (2006) concerns the presence of rainy and non-rainy periods, illustrated by rising and falling sequences in the polygons (Rule (e) in Table 2). We here clarify this interpretation by considering the direction of time around the polygons to inform about inter-annual variation in the monthly runoff coefficient: a clockwise loop generally has larger runoff to precipitation ratios on the rising sequence than on the falling sequence, while the reverse is true for a anticlockwise loop. Rules (f), (g) and (h) concern the variability of the precipitation–runoff behaviour from month to month, and they are mainly associated with the overall polygon area and the overall orientation (slope) of the polygon shape. Lastly, while we do not believe that runoff coefficients can be derived straightforwardly from the polygons, useful information can be obtained with regard to the mean monthly water balance computed across all 12 calendar months.

Table 2 Original and revised process interpretations associated with monthly precipitation–runoff polygons (with runoff plotted on the *y*-axis).

	Original process interpretations	Revised process interpretations
(a)	The length of each polygon side (segment) indicates the change in precipitation and runoff values for consecutive months.	The lengths and slopes of the polygon sides indicate the change in average values of precipitation or runoff for consecutive months.
(b)	The slope of each polygon side with respect to the vertical and horizontal axes shows the relative proportion of the precipitation and runoff that make up the runoff coefficient.	The slopes of the polygon sides indicate the difference in runoff between months relative to the difference in precipitation between months.
(c)	All the sides joined together (perimeter) form a closed polygon showing the catchment water balance over a full year.	The centroid of the polygon indicates the average mean monthly water balance, while the vertical distance of the centroid to the runoff–precipitation line indicates the average depth of monthly precipitation that becomes runoff.
(d)	Runoff is assumed to change linearly with precipitation over each month. Hence, the narrower a polygon is, the more linear the precipitation–runoff relationship is at the monthly and annual time scales. In contrast, a wider polygon signals a precipitation–runoff relationship that is linear at the monthly time scale but strongly non-linear at the annual time scale.	A narrow polygon indicates a more consistent monthly runoff–precipitation relationship between months, while a wide polygon indicates substantial between-month differences in the monthly runoff–precipitation relationship that may reflect such factors as evapotranspiration and storage retention and release of precipitation.
(e)	Each polygon has a sequence of rising and falling segments representing rainy and dry periods during the year, respectively. Runoff coefficients along rising sequences are often (but not always) greater than those along falling sequences; even though falling sequences signal non-rainy periods, they might be associated with sustained baseflow contributions, thus causing the runoff coefficient to take values greater than 1. Catchments with runoff coefficients greater than 1 are usually characterized by periods when the catchment is fed by baseflow and/or snowmelt in addition to precipitation.	Each polygon has a sequence of rising and falling sides representing periods when monthly runoff and precipitation are progressively increasing and decreasing, respectively. The direction of the hysteresis loop formed by the polygon provides information on inter-annual variation in the monthly runoff coefficient: a clockwise loop generally has larger runoff: precipitation ratios on the rising sequence than on the falling sequence, while the reverse is true for a anticlockwise loop.
(f)	Smaller polygon surface areas reflect constant monthly runoff coefficient and precipitation values.	Smaller polygon areas indicate more consistent monthly runoff, precipitation and runoff coefficients.
(g)	The smaller the overall slope of the polygon with respect to the horizontal axis, the more precipitation is converted into runoff.	The greater the overall slope of the polygon with respect to the horizontal axis, the more precipitation is converted into runoff.
(h)	The points at which a horizontal line intersects the polygon show the upper and lower limits of predicted runoff depths for a given precipitation depth. Conversely, the points at which a vertical line intersects the polygon show the upper and lower limits of precipitation that might give rise to a certain runoff value.	Horizontal line intersections with the polygon provide the lower and upper limits and range of mean monthly runoff, while vertical line intersections depict the upper and lower limits as well as the range of mean monthly precipitation that might give rise to a given mean monthly runoff depth.

This overall mean corresponds to the barycentre of the geometric shape; hence, we rephrased Rule (c) (Table 2) to reflect the fact that the centroid of the polygon indicates the average mean monthly water balance, while the vertical distance of the centroid to the runoff–precipitation line indicates the average depth of monthly precipitation that becomes runoff.

3.3 Polygon metrics

The complexity of the different polygon geometries was visually assessed by classifying the polygon shapes as convex (i.e. every internal angle in the polygon is less than or equal to 180°), concave (i.e. re-entrant or with a least one interior angle greater than 180°) and/or self-intersecting. Quantitatively, the polygons were characterized using the metrics outlined in Table 3. These metrics describe the shape, orientation and overall appearance of each monthly precipitation–runoff polygon and can all be associated with one of the process interpretations reported in Table 2. Briefly, the length of each polygon was computed along the long axis (i.e. the longest line within the polygon), while the width was computed as the longest line within the polygon normal to the length. The width measurement was used to differentiate narrow from wide polygons; the former illustrate linear precipitation–runoff behaviour, whereas the latter signal nonlinear precipitation–runoff transformations (Interpretation (d) in Table 2). The polygon surface area was estimated by overlaying a centimetre grid on each polygon. The length and slope of each segment within a polygon were also measured, while the overall orientation

Table 3 Quantitative metrics associated with the monthly precipitation–runoff polygon. The polygon process interpretations numbered (a)–(h) are reported in full in Table 2.

Metric	Abbreviation	Process interpretation identifier
Length of each segment	SL-months	A
Slope of each segment	SS-months	B
Centroid (coordinates)	C_x, C_y	c
Polygon length (along *x*-axis)	Length	d
Polygon width (along *y*-axis)	Width	d
No. of rising precipitation and runoff segments	RisingS	e
No. falling precipitation and runoff segments	FallingS	e
Direction of the polygon with time	Direction	e
Surface area	Area	f
Overall orientation of polygon (based on regression slope, $y = mx + c$)	Orientation	g
—	—	h

of a polygon (with respect to the *x*-axis) was approximated by the slope of a linear regression line fit through the 12 points on each diagram. The number of rising and falling segments against the *x*-axis (precipitation) and *y*-axis (runoff) was obtained by visually assessing each segment within a polygon. The coordinates C_x and C_y of the centroid of each polygon were approximated using the following formulas:

$$C_x = \frac{1}{6A}\sum_{i=1}^{11}(x_i + x_{i+1})\cdot(x_i \cdot y_{i+1} - x_{i+1} \cdot y_i) \qquad (1)$$

$$C_y = \frac{1}{6A}\sum_{i=1}^{11}(y_i + y_{i+1})\cdot(x_i \cdot y_{i+1} - x_{i+1} \cdot y_i) \qquad (2)$$

where A is the area of the polygon, x_i is the precipitation value for month i, and y_i is the runoff value for month i. Lastly, polygons were attributed a value of +1 when their direction of time was strictly anticlockwise, –1 when their direction of time was strictly clockwise, and 0 when one or more changes of direction were present. Process interpretation (h) can be considered as a visual way to identify minimum and maximum values of monthly precipitation and monthly discharge for a given site; because the minimum and maximum values are descriptive statistics and not polygon metrics per se, process interpretation (h) was not matched with any metric in Table 3.

Values of the polygon metrics were compared among the 10 North-Watch catchments using principal component analysis (PCA) to reduce the number of dimensions for comparison among the polygon variables. Four different PCAs were run in order to examine the potential of different subsets of quantitative metrics, polygon-based or not, to explain the variability among the sites. In the first PCA, the runoff coefficients obtained for each month were used as input variables and acted as a reference framework for the comparison of precipitation–runoff behaviour. Monthly runoff coefficients were simply computed as the ratio of runoff to precipitation for each month. Subsequently, three different subsets of polygon metrics were used as input variables in a PCA to evaluate their relative efficiency at matching or exceeding the amount of variance explained by the monthly runoff coefficients. Hence, in the second PCA, all polygon metrics (Table 3) were entered as variables. The third PCA included all quantitative metrics, but excluded the slopes and lengths of the 12 segments of each polygon. Lastly, in the fourth PCA, only segment slopes and lengths of the polygons were used as input data. In order to compare all four PCAs, the top three or four eigenvectors that contributed most to the first two principal components (PC1 and PC2) were examined. All analyses were performed using SigmaPlot (Systat Software Inc.) and MINITAB (Minitab Inc., USA).

4 RESULTS

Average monthly runoff coefficients (expressed in per cent) for the Girnock and Strontian catchments were distinct from the others (Table 4) in that they never exceeded 100%. In contrast, all other catchments were characterized by at least one or two months during which the computed runoff coefficient exceeded 100%, thus suggesting contributions of baseflow and/or snowmelt (Table 5) to streamflow.

Table 4 Average monthly and annual precipitation (*P*, mm), discharge (*Q*, mm) and runoff coefficients (RC, %) for the 10 North-Watch sites. The computed figures are based on 10-year analyses except for two catchments (refer to text for details).

Catchment	Variable	Jan.	Feb.	Mar.	Apr.	May	Jun.	Jul.	Aug.	Sep.	Oct.	Nov.	Dec.	Annual
Allt a'Mharcaidh	*P*	94.4	80.0	109.6	78.5	69.9	123.6	76.8	119.3	139.3	163.3	103.0	64.1	1221.6
	Q	103.9	94.4	112.5	67.9	66.9	54.6	42.0	41.8	49.3	86.0	69.8	84.7	873.6
	RC	110%	118%	103%	86%	96%	44%	55%	35%	35%	53%	68%	132%	72%
Girnock	*P*	99.9	66.5	70.9	85.6	67.4	63.2	76.0	91.0	71.1	148.7	120.2	98.2	1058.8
	Q	86.4	58.5	52.4	49.0	28.9	19.8	24.9	32.9	25.0	73.2	75.4	76.8	603.2
	RC	86%	88%	74%	57%	43%	31%	33%	36%	35%	49%	63%	78%	57%
Strontian	*P*	309.9	299.8	215.1	158.2	101.4	162.8	182.6	154.3	197.3	284.5	271.6	294.5	2632.0
	Q	281.6	243.3	194.4	132.1	55.8	122.0	128.7	120.2	150.7	273.8	246.6	263.7	2213.0
	RC	91%	81%	90%	84%	55%	75%	70%	78%	76%	96%	91%	90%	84%
Catamaran	*P*	61.1	70.6	97.0	80.8	73.7	58.2	97.1	76.2	92.8	110.0	86.4	86.4	990.2
	Q	18.0	11.0	30.8	146.9	120.1	27.0	16.2	17.6	12.7	35.6	49.2	50.0	535.0
	RC	30%	16%	32%	182%	163%	46%	17%	23%	14%	32%	57%	58%	54%
Dorset	*P*	94.6	57.0	58.0	52.4	76.0	91.7	97.5	76.3	110.1	94.8	107.3	64.8	980.4
	Q	36.7	19.1	56.0	155.1	58.5	24.6	21.7	10.6	19.8	74.2	67.6	32.9	576.7
	RC	39%	33%	97%	296%	77%	27%	22%	14%	18%	78%	63%	51%	59%
Wolf Creek	*P*	28.6	20.2	19.1	16.1	28.4	58.1	81.3	70.3	53.1	40.2	36.7	27.8	479.8
	Q	9.0	6.7	5.7	5.0	44.9	101.7	56.2	41.4	32.7	21.9	15.2	11.7	352.2
	RC	31%	33%	30%	31%	158%	175%	69%	59%	62%	54%	42%	42%	73%
Krycklan	*P*	45.3	39.5	31.8	31.0	42.1	59.9	92.5	89.5	62.3	62.4	52.6	42.5	651.2
	Q	9.6	5.5	5.7	51.7	81.2	21.4	20.5	33.6	29.7	24.8	24.1	19.0	326.7
	RC	21%	14%	18%	167%	193%	36%	22%	38%	48%	40%	46%	45%	50%
HJ Andrews	*P*	365.1	191.6	232.7	150.7	138.2	77.6	12.1	21.5	65.6	175.0	304.8	423.5	2158.3
	Q	289.2	162.2	229.8	226.0	193.1	95.1	31.1	16.9	15.9	41.2	152.3	291.6	1744.4
	RC	79%	85%	99%	150%	140%	123%	258%	78%	24%	24%	50%	69%	81%
Hubbard Brook	*P*	101.6	76.1	101.0	111.0	124.8	129.7	106.4	128.1	130.2	128.6	132.1	112.1	1381.5
	Q	61.3	30.8	119.5	180.0	91.2	57.8	18.2	25.7	39.5	73.0	101.7	83.4	882.2
	RC	60%	41%	118%	162%	73%	45%	17%	20%	30%	57%	77%	74%	64%
Sleepers	*P*	110.5	72.7	99.4	95.4	113.6	109.7	129.6	108.8	115.4	100.1	109.8	91.1	1256.1
	Q	42.9	26.6	61.7	223.6	118.3	51.3	31.4	22.5	16.9	35.7	57.9	54.8	743.7
	RC	39%	37%	62%	234%	104%	47%	24%	21%	15%	36%	53%	60%	59%

Table 5 Average actual evapotranspiration rate (AET, mm d^{-1}) and monthly snow water equivalent (SWE, mm) for the 10 North-Watch sites. AET values are taken from Carey *et al.* (2010). SWE values were estimated using a single degree-day model across all sites, i.e. snowfall is inferred from precipitation at below-zero temperatures, and the snowpack melted with a degree-day factor of 4 when air temperatures are above 0°C.

Catchment	Variable	Jan.	Feb.	Mar.	Apr.	May	Jun.	Jul.	Aug.	Sep.	Oct.	Nov.	Dec.
Allt a'Mharcaidh	AET	0.21	0.46	0.85	1.51	1.96	1.98	1.49	0.95	0.59	0.37	0.20	0.14
	SWE	3.78	3.40	9.30	4.70	0.60	0.00	0.00	0.00	0.00	0.75	2.28	1.50
Girnock	AET	0.22	0.38	0.71	1.26	2.10	2.85	2.92	2.10	1.26	0.64	0.30	0.17
	SWE	26.40	19.95	13.72	3.94	0.25	0.00	0.00	0.00	0.00	1.05	6.22	14.85
Strontian	AET	0.22	0.40	0.73	1.30	2.04	2.70	2.50	1.77	1.08	0.57	0.27	0.16
	SWE	3.38	0.00	0.00	0.00	0.00	0.00	0.00	0.00	0.00	0.00	5.51	0.00
Catamaran	AET	0.11	0.25	0.61	1.31	3.01	4.95	5.18	3.92	2.12	0.81	0.32	0.13
	SWE	6.28	39.77	140.55	86.05	0.00	0.00	0.00	0.00	0.00	0.00	15.80	9.06
Dorset	AET	0.07	0.14	0.35	0.85	1.86	2.97	2.94	2.14	1.14	0.49	0.17	0.07
	SWE	11.07	24.42	103.87	95.36	3.60	0.00	0.00	0.00	0.00	3.31	17.35	12.45
Wolf Creek	AET	0.03	0.06	0.12	0.28	0.57	0.96	0.94	0.67	0.32	0.14	0.05	0.03
	SWE	2.28	1.44	1.44	57.16	90.54	0.00	0.00	0.00	6.77	11.63	3.50	3.76
Krycklan	AET	0.08	0.15	0.32	0.72	1.41	2.34	2.50	1.67	0.85	0.36	0.14	0.07
	SWE	9.62	12.18	44.02	89.70	9.60	0.00	0.00	0.00	0.00	5.42	10.48	19.09
HJ Andrews	AET	0.17	0.30	0.55	0.97	1.72	2.49	2.94	2.22	1.26	0.57	0.24	0.12
	SWE	69.30	68.30	19.60	4.22	0.00	0.00	0.00	0.00	0.00	0.00	10.82	70.28
Hubbard Brook	AET	0.10	0.20	0.47	1.07	2.25	3.55	3.62	2.67	1.47	0.59	0.23	0.10
	SWE	19.62	33.66	121.87	97.63	0.33	0.00	0.00	0.00	0.00	1.26	13.77	22.96
Sleepers	AET	0.10	0.20	0.46	1.03	2.38	3.81	3.74	2.61	1.49	0.63	0.24	0.10
	SWE	11.99	14.39	74.21	205.30	1.76	0.00	0.00	0.00	0.00	3.30	9.17	11.50

The months associated with runoff coefficients over 100% were highly variable among the sites (e.g. March–April for the Hubbard Brook site, April for the Dorset site, April–May for the Catamaran, Krycklan and Sleepers River sites, and May–June for the Wolf Creek site). Both the Allt a'Mharcaidh and the HJ Andrews sites showed four successive months with runoff coefficients in excess of 100% (December–March and April–July, respectively).

Precipitation–runoff polygons for each catchment are shown in Fig. 3. For each catchment, all polygon metrics, except the length and slope of the 12 polygon segments, are also shown in Table 6. Overall, the catchments were characterized by rather wide polygons (i.e. polygons with relatively large width measurements); one exception was the Strontian site associated with a narrower polygon (i.e. small width measurement, Table 6). With regard to the other polygon shape metrics, the 10 North-Watch sites appeared to exhibit distinct hydrological behaviours. For instance, the polygons for the HJ Andrews and Wolf Creek sites had a convex shape, while the polygons for all other sites were concave. The concave polygons were sometimes self-intersecting at one or several locations. For the Krycklan, HJ Andrews and Wolf Creek sites, the polygons were the most widely spread along both axes (precipitation and runoff). In contrast, for the Sleepers River site, a wide range of monthly runoff values was associated with a much smaller range of monthly precipitation values.

The results of the four PCAs are illustrated in Fig. 4, and their corresponding eigenvectors that contribute most to the first two principal components (PC1 and PC2) are presented in Table 7. The focus on PC1 and PC2 only was motivated by the observation of scree plots (not shown), which revealed that the first two principal components explained the greatest amount of variability among the catchments. With the PCA shown in Fig. 4(a) used as the reference framework, the most important variables explaining 68.4% of the variance among the 10 study catchments were the runoff coefficients for winter months (41.2%) followed by those for summer months (27.2%) (Table 7). The PCAs in Fig. 4(b) and 4(d) explained only 45.4% and 39.9% of the variance, respectively. Interestingly, the PCA in Fig. 4(c) explained 69.5% of the variance among the study catchments, thus equalling the variance explained in the PCA of Fig. 4(a). This suggests that all polygon metrics, except those which were segment-based (i.e. slopes and lengths), are as informative as monthly average runoff coefficients when it comes to capturing the variability in precipitation–runoff behaviour. In the PCA shown in Fig. 4(c), PC1s explanation of 36.8% of the variance largely reflected the number of rising and falling sequences of precipitation and runoff and the width of

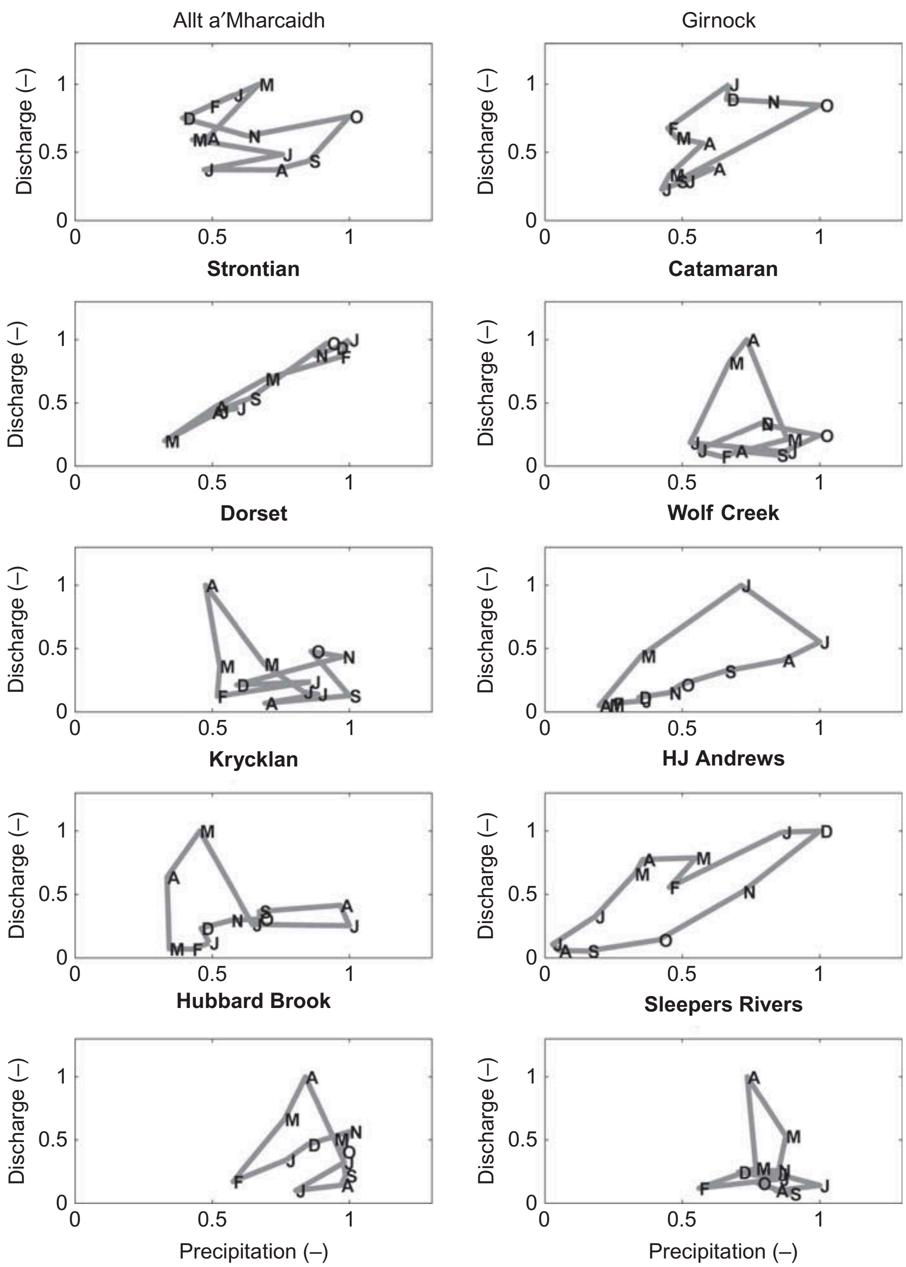

Fig. 3 Monthly precipitation–runoff polygons for the 10 North-Watch sites. Note that precipitation and runoff values have been standardized so that they can potentially range from 0 to 1. Letters J to D on the polygon vertices represent calendar months.

the polygons, whereas PC2 was correlated with the coordinates of the centroid and the direction of the polygons.

5 DISCUSSION

5.1 Insights on catchment behaviour and seasonality

Monthly precipitation–runoff polygons associated with qualitative process interpretations and quantitative shape metrics provided a quick, efficient way to compare the hydrological dynamics prevailing in different mid- to high-latitude catchments. Although it might seem crude, the use of monthly data for such an exercise was motivated by the fact that the main focus was on seasonality patterns. Most of the North-Watch sites have a snow-dominated portion of their hydrographs that is apparent over several months of the year and can be contrasted with variable summer drought effects. Across the 10 North-Watch sites, the polygon associated with the Strontian site was the only one resembling a straight line (Fig. 3). Indeed, all catchments but Strontian were associated with wide polygons (Table 6, Fig. 3),

Table 6 Selected polygon metrics associated with the 10 studied catchments. Values are standardized and unitless. Refer to Table 3 for the specific definitions of the polygon metrics.

Catchment	Area	Orientation	C_x	C_y	No. of rising segments	No. of falling segments	Length	Width	Direction
Allt a'Mharcaidh	0.12	–0.10	0.47	0.27	6	6	0.63	0.61	Anticlockwise
Girnock	0.15	0.39	0.66	0.67	6	6	0.77	0.58	Anticlockwise
Strontian	0.03	0.83	–0.06	–0.08	5	7	0.8	0.07	Mixed
Catamaran	0.14	0.01	1.13	0.60	5	7	0.93	0.47	Anticlockwise
Dorset	0.14	–0.25	–0.15	–0.23	7	5	0.93	0.52	Mixed
Wolf Creek	0.31	0.65	–0.61	–0.51	4	8	0.95	0.8	Clockwise
Krycklan	0.20	–0.01	0.29	0.16	5	7	0.93	0.66	Mixed
HJ Andrews	0.32	0.74	0.48	0.49	6	6	0.95	0.97	Anticlockwise
Hubbard Brook	0.11	0.04	–0.48	–0.41	7	5	0.9	0.42	Mixed
Sleepers River	0.09	–0.06	–0.78	–0.41	6	6	0.92	0.44	Mixed

which means that their response to precipitation varies from month to month and is highly variable on an annual basis (refer to process interpretation (d) in Table 2). The Strontian exception is consistent with a previous study which demonstrated that, among all North-Watch sites, catchment storage is the least variable temporally at Strontian due to the high precipitation all year round (Carey *et al*. 2010), warmer temperatures that prevent the storage of winter precipitation as snow, and the absence of large lakes or other reservoirs. Hence, the catchment does not need to overcome a seasonal storage deficit to produce runoff, which explains the strong linear relationship between precipitation and runoff at both the monthly and the annual time scales.

One of the striking features of the polygons was the presence of horizontal segments, which are illustrative of periods when precipitation changes do not result in significant runoff changes; these could be due to significant amounts of precipitation going to storage as snow accumulation, detention storage, soil moisture or other fluxes such as evapotranspiration and groundwater recharge. Horizontal polygon segments could be identified for different sites, although they are not attributable to similar processes: high evaporation dynamics are likely to be responsible for horizontal segments during the summer months (e.g. June–July at the Krycklan site, July–August at the Allt a'Mharcaidh and Catamaran sites, and August–September at the HJ Andrews site), while snow accumulation and groundwater recharge are rather presumed in the winter months (e.g. December–January at the HJ Andrews and the Dorset sites, October–November and February–March at the Krycklan site).

The polygons which are the most widely spread along both the precipitation and the runoff axes signal catchments with distinct wet and dry seasons in both precipitation and runoff; this is the case for the Krycklan, HJ Andrews and Wolf Creek sites, and this observation is consistent with Carey *et al.* (2010). In contrast, the Catamaran, Sleepers River, Hubbard Brook and Dorset sites show high seasonality in runoff in spite of a relatively low seasonality in precipitation. For example, the Sleepers River site was associated with a "column-like" polygon, with a large range of monthly runoff values but a much smaller range of monthly precipitation values; this is consistent with the explanation provided by Carey *et al.* (2010) in terms of this catchment's higher damping of the precipitation input and greater hydrological resistance—that is the degree to which runoff is decoupled/desynchronized with precipitation—due to increased storage. However, because very different and irregular polygon shapes were present among the 10 sites, visual assessment alone did not permit the extension of this interpretation in terms of which catchments behave alike. Thus, quantitative polygon shape metrics (Table 3) and PCA were used to examine the differences between the catchments and explore overall similarities among them.

5.2 Polygon metrics for catchment inter-comparison

The PCA based on all polygon metrics but those which are segment-based (Fig. 4(c)) explained a similar amount of variance to the reference PCA involving monthly average runoff coefficients (Fig. 4(a)). This seems to suggest that the subset of polygon metrics used in Fig. 4(c) is as informative as runoff coefficients used in isolation. The polygon methodology, however, offers a significant advantage compared to runoff coefficients in that the process interpretation rules listed in Table 2 and the positioning of the different catchments in the ordination space (Fig. 4), can be used to better understand the

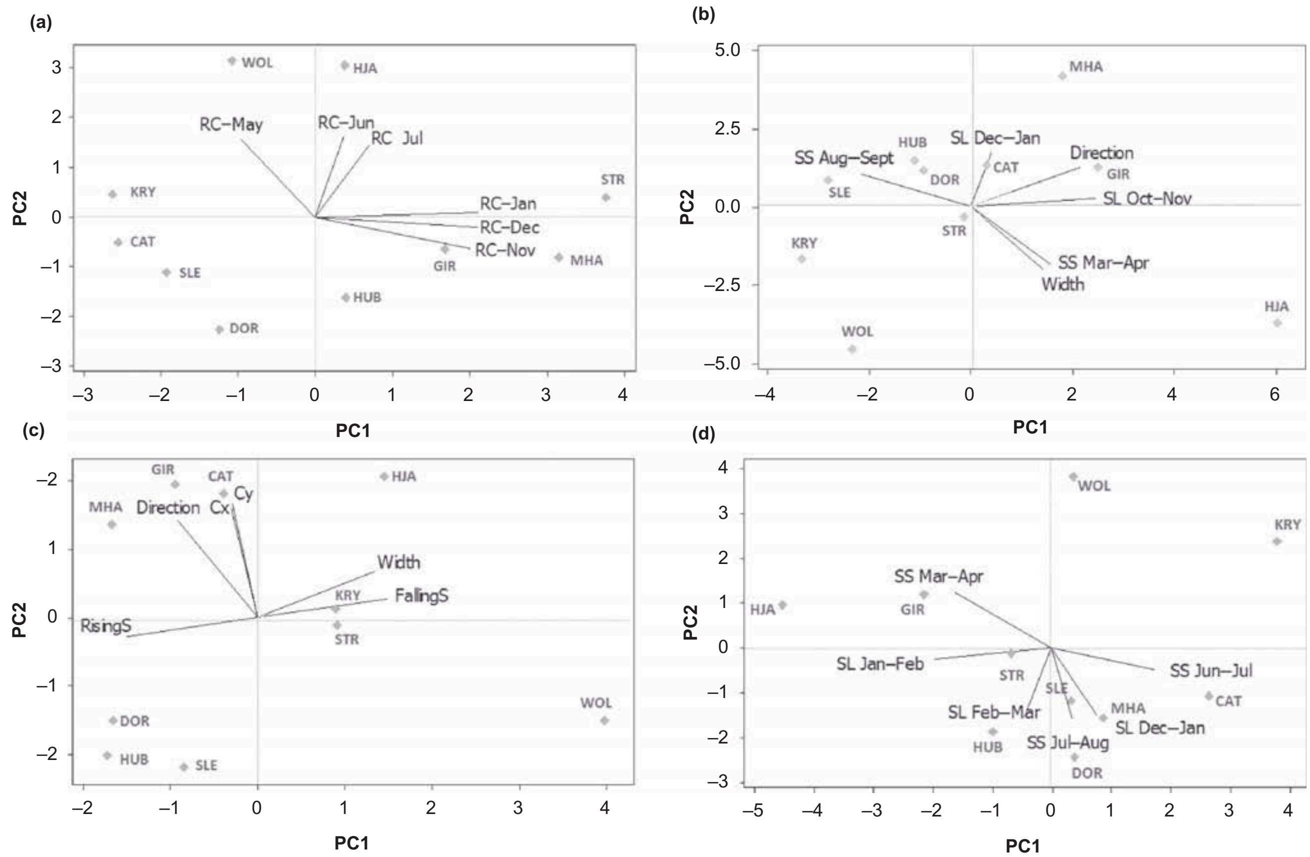

Fig. 4 Bi-plot showing the magnitude and sign of each polygon metric's contribution (PCA coefficients or loadings) to the first two principal components with the individual scores for each of the 10 North-Watch sites. PC1 and PC2 are the first and the second principal components, respectively. RC refers to the average monthly runoff coefficient for the corresponding month. The PCAs involved: (a) monthly runoff coefficients only; (b) all quantitative polygon metrics listed in Table 3; (c) all quantitative polygon metrics except those which are segment-based (slopes and lengths); (d) segment-based (slopes and lengths) polygon metrics only. In all panels, distances between points are an approximation of their similarity, but angles between variables (black lines) cannot be interpreted as an approximation of their inter-correlation.

Table 7 Selected characteristics of the four PCAs illustrated in Fig. 4. For each panel (a)–(d) in Fig. 4, the top three or four variables that contribute most to the first two principal components (PC1 and PC2) are reported. Percentages in the second last row show the variance individually explained by PC1 or PC2 while percentages in the last row illustrate the total variance explained by the first two principal components. Refer to Table 3 for the meaning of the abbreviated polygon-metric names.

Fig. 4(a)		Fig. 4(b)		Fig. 4(c)		Fig. 4(d)	
PC1	PC2	PC1	PC2	PC1	PC2	PC1	PC2
RC-Dec	RC-Jun	SL Oct–Nov	Width	RisingS	C_x	SL Jan–Feb	SS July–Aug
RC-Jan	RC-Jul	SS Aug–Sep	SS Mar–Apr	FallingS	C_y	SS June–Jul	SL Feb–Mar
RC-Feb	RC-Aug	Direction	SL Dec–Jan	Width	Direction	SS Mar–Apr	SL Dec–Jan
41.2%	27.2%	24.4%	21.0%	36.8%	32.7%	22.7%	17.2%
68.4%		45.4%		69.5%		39.9%	

precipitation–runoff coupling. In Fig. 4(c), sites in the lower-left quadrant of the PCA space (i.e. Dorset, Hubbard Brook and Sleepers River) were characterized by polygons that were not strictly clockwise or anticlockwise (i.e. mixed direction, Table 6), a property which suggests that, although those catchments have less variance in their precipitation input (i.e. lower seasonality in precipitation), they are nevertheless subjected to important runoff variability (i.e. high seasonality in runoff) due to their storage dynamics and their seasonality in potential evapotranspiration (e.g. Shanley *et al.* 2002, Buttle and Eimers 2009, Detty and McGuire 2010). The Catamaran, Girnock, Allt a'Mharcaidh and HJ Andrews (e.g. Soulsby *et al.* 2000, Caissie *et al.* 2002, Tetzlaff *et al.* 2007, 2009) polygons were mostly anticlockwise (Table 6), hence their positioning in the two upper PCA quadrants. However, the first three catchments stood apart (left upper quadrant), given the larger coordinates of their polygon centroids and therefore their greater ability to convert a large proportion of precipitation into runoff on a monthly basis (process interpretation (c), Table 2). The Wolf Creek catchment was isolated from all the others in the PCA space, mainly because of the clockwise direction with time (Table 6), and this can be explained by the low temperature, widespread presence of permafrost, small annual precipitation and considerable influence of snowmelt prevailing in the region (e.g. Carey and Woo 2001).

While the PCA results obtained here rely on a rather small sample size and cannot be easily assessed for statistical significance, they can nevertheless be compared to those obtained by Carey *et al.* (2010) with the same ensemble of catchments; the PCA then included a range of normalized fluxes and standard flow metrics which explained similar variance (74%) among the 10 North-Watch sites. This proportion of explained variance is slightly superior to that associated with the best subset of polygon metrics (69.5%), or the reference PCA with runoff coefficients (68.4%) developed in the current paper. Carey *et al.* (2010) also found that catchments which are geographically close to one another (e.g. Sleepers River, Hubbard Brook, Catamaran and Dorset or Girnock, Strontian and Mharcaidh) clustered together in the ordination space, but, while this was true for the PCA based on runoff coefficients (Fig. 4(a)), it was not the case for the PCA based on all polygon metrics, except those segment-based (Fig. 4(c)). As for the segment-based polygon metrics, they introduced a significant amount of noise in the data set as the PCAs in Fig. 4(b) and (d) were associated with explained amounts of variance that were significantly lower than the PCAs in Fig. 4(a) and (c). It is worth mentioning, however, that this PCA exercise was conducted by lumping 4–10 years of data for each study catchment; it is not expected that the catchments would group in a similar fashion if the monthly precipitation and discharge values had been computed separately for average years, drier-than-average years and wetter-than-average years.

5.3 Drawbacks of the suggested polygon methodology

One of the drawbacks of this study was the absence of actual snowpack and snow water equivalent (SWE) measurements: estimates were included in Table 5 for illustration purposes, but excluded from the polygon and statistical analyses as their accuracy cannot be verified; for example, the same degree-day model was applied to all 10 catchments for the estimation of SWE values, while it is unlikely that the same degree-day factor should be used for all catchments. While runoff coefficients above 100% can signal the contribution of baseflow and/or snowmelt to streamflow (Kadioglu and Sen 2001, Sen and Altunkaynak 2006), it was not always possible to assess whether higher runoff coefficient values could be attributed to both sources simultaneously or only one of the two. It was also rather peculiar that the HJ Andrews site had four successive months with runoff coefficients in excess of 100% (March–July). This might be attributed to the melting of the snowpack until May in this climatic region, and then to the fact that during the dry summer season, the runoff coefficient is made of sustained baseflow divided by virtually no rainfall input in the presence of non-negligible evapotranspiration (Likens and Bormann 1995).

One of the difficulties associated with the methodology presented here had to do with the complex shapes of some polygons. Indeed, while most of the polygons in the previously published papers (Kadioglu and Sen 2001, Sen and Altunkaynak 2006) were predominantly convex ("simple polygons"), eight out of the 10 polygons in this study across mid- to high-latitude catchments are concave, self-intersecting at one or several locations and sometimes overlapping as well. This similarity might reflect similar runoff dynamics, which are either snowmelt-driven or rainfall-driven depending on the season. The self-intersecting points caused some difficulty in calculating the surface area of the polygons, as the question of whether overlapping polygon portions should be counted once or twice while computing the polygon area had to be resolved. In the end, the area of overlapping polygon portions was taken into account twice so as to use a similar methodology for both concave and convex shapes. The self-intersecting points also made it difficult not only to compute the coordinates of the polygon centroids but also to estimate the direction of the polygons with time. In additional analyses not shown here, the presence or absence of self-intersecting vertices in the polygons was codified as a binary variable to be included in the PCAs of Fig. 4 (b) and 4(c); however, this binary variable added noise to the data set and did not contribute to increase the amount of explained variance. These problems are specific to the polygon methodology, but they do not dismiss the relevance of that methodology for seasonality analysis for site comparison in different geographic and climatic regions.

6 CONCLUSION

Quantitative metrics describing the shape of monthly precipitation–runoff polygons were compared to assess their ability to discriminate the different seasonality patterns present among 10 mid- to high-latitude catchments within the North-Watch project. In terms of explained variance, some polygon quantitative metrics were as effective as monthly average runoff coefficients in illustrating the differences between the 10 North-Watch sites. The use of polygons has a significant advantage over the use of simple monthly average runoff coefficients, since the former were useful to look at the dynamics prevailing in specific months and achieve a better assessment of the coupling between precipitation and runoff and the relative degree of seasonality. This polygon methodology, once linked with a range of quantitative metrics, provides a simple tool for understanding and comparing catchment functioning, not only from an annual water balance point of view but also from a monthly-to-seasonal perspective. Given the relatively wide availability of precipitation and runoff data for past periods (e.g. historical records) and also for future years (e.g. prediction models), it is suggested that these polygons could help improve assessment of the impacts of water use or climate change in environments where hydrological response varies at different time scales.

Acknowledgements Special thanks go to Rick Cunjak and Daniel Caissie for their support in providing the data for Catamaran Brook. The authors are also grateful to those individuals and funding agencies who contributed to gathering the data set presented in this paper.

Funding The North-Watch project (http://www.abdn.ac.uk/northwatch/) is funded by the Leverhulme Trust (F/00 152/AG).

REFERENCES

Anderson, N.H., 1992. Influence of disturbance on insect communities in Pacific Northwest streams. *Hydrobiologia*, 248, 79–92.

Bailey, A.S., *et al.*, 2003. *Hydrometeorological database for Hubbard Brook Experimental Forest: 1955–2000*. NE Research Station General Technical Report NE-305. Newtown Square, PA: USDA Forest Service, 36 p.

Bartolini, E., *et al.*, 2011. Runoff regime estimation at high-elevation sites: a parsimonious water balance approach. *Hydrology and Earth System Sciences*, 15, 1661–1673.

Bayfield, N.G. and Nolan, A.J., 1998. Vegetation and soils of the Allt a'Mharcaidh catchment, Cairngorm mountains. *Scottish Geographical Magazine*, 114, 18–21.

Bouchard, M. and Jolicoeur, S., 2000. Chemical weathering studies in relation to geomorphological research in southeastern Canada. *Geomorphology*, 32, 213–238.

Burn, D.H., 1997. Catchment similarity for regional flood frequency analysis using seasonality measures. *Journal of Hydrology*, 202, 212–230.

Buttle, J.M. and Eimers, M.C., 2009. Scaling and physiographic controls on streamflow behaviour on the Precambrian Shield, south-central Ontario. *Journal of Hydrology*, 374, 360–372.

Caissie, D., *et al.*, 2002. Comparison of streamflow between pre and post timber harvesting in Catamaran Brook (Canada). *Journal of Hydrology*, 258, 232–248.

Carey, S.K., *et al.*, 2010. Inter-comparison of hydro-climatic regimes across northern catchments: synchronicity, resistance and resilience. *Hydrological Processes*, 24, 3591–3602.

Carey, S.K. and Quinton, W.L., 2005. Evaluating runoff generation during summer using hydrometric, stable isotope and hydrochemical methods in a discontinuous permafrost alpine catchment. *Hydrological Processes*, 19, 95–114.

Carey, S.K. and Woo, M.K., 2001. Slope runoff processes and flow generation in a subarctic, subalpine catchment. *Journal of Hydrology*, 253, 110–129.

Castellarin, A., Burn, D.H., and Brath, A., 2001. Assessing the effectiveness of hydrological similarity measures for flood frequency analysis. *Journal of Hydrology*, 241, 270–285.

Detty, J.M. and McGuire, K.J., 2010. Topographic controls on shallow groundwater dynamics: implications of hydrologic connectivity between hillslopes and riparian zones in a till mantled catchment. *Hydrological Processes*, 24, 2222–2236.

Eimers, M.C., Watmough, S.A., and Buttle, J.M., 2008. Long-term trends in dissolved organic carbon concentration: a cautionary note. *Biogeochemistry*, 87, 71–81.

Hoyt, W.G., 1936. Studies of relations of rainfall and runoff in the United States. *US Geological Survey Water-Supply Paper 772*.

Jothityangkoon, C. and Sivapalan, M., 2009. Framework for exploration of climatic and landscape controls on catchment water balance, with emphasis on inter-annual variability. *Journal of Hydrology*, 371, 154–168.

Kadioglu, M. and Şen, Z., 2001. Monthly precipitation–runoff polygons and mean runoff coefficients. *Hydrological Sciences Journal*, 46, 3–11.

Kruitbos, L.M., *et al.*, 2012. Hydroclimatic and hydrochemical controls on Plecoptera (stonefly) diversity and distribution in northern freshwater ecosystems. *Hydrobiologia*, doi:10.1007/s10750-012-1085–1.

La Torre Torres, I.B., *et al.*, 2011. Seasonal rainfall–runoff relationships in a lowland forested watershed in the southeastern USA. *Hydrological Processes*, 25, 2032–2045.
Laaha, G. and Blöschl, G., 2006. Seasonality indices for regionalizing low flows. *Hydrological Processes*, 20, 3851–3878.
Laudon, H., *et al.*, 2011. Patterns and dynamics of dissolved organic carbon (DOC) in boreal streams: the role of processes, connectivity, and scaling. *Ecosystems*, 14, 880–893. doi:10.1007/s10021-011-9452-8.
Likens, G.E. and Bormann, F.H., 1995. *Biogeochemistry of a forested ecosystem.* 2nd ed. New York: Springer-Verlag.
McCartney, S.E., Carey, S.K., and Pomeroy, J.W., 2006. Intra-basin variability of snowmelt water balance calculations in a subarctic catchment. *Hydrological Processes*, 20, 1001–1016.
Parajka, J., *et al.*, 2009. Comparative analysis of the seasonality of hydrological characteristics in Slovakia and Austria. *Hydrological Sciences Journal*, 54, 456–473.
Pardé, M., 1947. *Fleuves et rivières.* 2nd ed. Paris: Colin.
Robins, N.S., 1990. *Hydrogeology of Scotland*. London: HMSO.
Şen, Z. and Altunkaynak, A., 2006. A comparative fuzzy logic approach to runoff coefficient and runoff estimation. *Hydrological Processes*, 20, 1993–2009.
Shanley, J.B., *et al.*, 2002. Controls on old and new water contributions to stream flow at some nested catchments in Vermont, USA. *Hydrological Processes*, 16, 589–609.
Shanley, J.B. and Chalmers, A., 1999. The effect of frozen soil on snowmelt runoff at Sleepers River, Vermont. *Hydrological Processes*, 13, 1843–1857.
Soulsby, C., *et al.*, 2000. Isotope hydrology of the Allt a' Mharcaidh catchment, Cairngorms, Scotland: implications for hydrological pathways and residence times. *Hydrological Processes*, 14, 747–762.
Tetzlaff, D., *et al.*, 2007. Conceptualization of runoff processes using a geographical information system and tracers in a nested mesoscale catchment. *Hydrological Processes*, 21, 1289–1307.
Tetzlaff, D., *et al.*, 2009. How does landscape structure influence catchment transit time across different geomorphic provinces? *Hydrological Processes*, 23, 945–953.
Tetzlaff, D., Soulsby, C., and Birkel, C., 2010. Hydrological connectivity and microbiological fluxes in montane catchments: the role of seasonality and climatic variability. *Hydrological Processes*, 24, 1231–1235.
Vidon, P., Hubbard, L.E., and Soyeux, E., 2009. Seasonal solute dynamics across land uses during storms in glaciated landscape of the US Midwest. *Journal of Hydrology*, 376, 34–47.
Western, A.W., Grayson, R.B., and Blöschl, G., 2002. Scaling of soil moisture: a hydrologic perspective. *Annual Review of Earth and Planetary Sciences*, 30, 149–180.
Wilson, D.J., Western, A.W., and Grayson, R.B., 2004. Identifying and quantifying sources of variability in temporal and spatial soil moisture observations. *Water Resources Research*, 40, W02507. doi:10.1029/2003WR002306.
Woods, R., 2003. The relative roles of climate, soil, vegetation and topography in determining seasonal and long-term catchment dynamics. *Advances in Water Resources*, 26, 295–309.
Xiong, L.H., Guo, S.L., and O'Connor, K.M., 2006. Smoothing the seasonal means of rainfall and runoff in the linear perturbation model (LPM) using the Kernel estimator. *Journal of Hydrology*, 324, 266–282.